Exp Brain Res (2003) 153: 530–542
DOI 10.1007/s00221-003-1671-6

RESEARCH ARTICLE

S. C. Bledsoe · S. E. Shore · M. J. Guitton

# Spatial representation of corticofugal input in the inferior colliculus: a multicontact silicon probe approach

Received: 16 November 2002 / Accepted: 7 July 2003 / Published online: 22 October 2003


**Abstract** The inferior colliculus (IC) is a well-established target of descending projections from the auditory cortex (AC). However, our understanding of these pathways has been limited by an incomplete picture of their functional influence within the three-dimensional space of the IC. Our goal was to study the properties and spatial representation of corticofugal input in the IC of guinea pigs with a high degree of spatial resolution. We systematically mapped neural activity in the IC using two types of silicon substrate probes that allow for simultaneous recording at multiple neural sites. One probe provided a high resolution in the dorsal-ventral plane and the other provided spatial resolution in the medial-lateral plane. Electrical stimulation of the ipsilateral AC produced excitatory responses in the IC with thresholds usually below 5–10 μA. First spike latencies were predominantly in the 6–20 ms range, although latencies from 3–5 ms were also observed. Broadly distributed unimodal spike patterns with modal latencies greater than 30 ms were occasionally seen. The excitatory responses to cortical stimulation were mostly unimodal and occasionally bimodal with a wide range of spike distribution patterns and response durations. Excitation was often followed by suppression of spontaneous activity. Suppression of acoustic responses was observed even when there was little or no response to electrical stimulation, suggesting spatial-temporal integration. A few of the responding neurons showed purely inhibitory responses to electrical stimulation, suggesting that there are disynaptic routes of corticocollicular inhibition. Detailed spatial mapping revealed that the response patterns and their durations had a characteristic spatial distribution in the IC.

**Keywords** Auditory · Corticofugal pathways · Single-unit physiology · Multiple-site recordings · Auditory cortex

S. C. Bledsoe (✉) · S. E. Shore
Kresge Hearing Research Institute, Dept. of Otolaryngology,
University of Michigan,
1301 E Ann St,
Ann Arbor, MI 48109, USA
e-mail: sbledsoe@umich.edu
Tel.: +1-734-7634341
Fax: +1-734-7640014

M. J. Guitton
INSERM, University of Montpellier,
Montpellier, France

## Introduction

The inferior colliculus (IC) is a key structure in the auditory system, playing a role in both normal hearing (Aitkin 1986) and spatial orientation to sound (Jane et al. 1965). Besides its critical role in the ascending auditory pathway, the IC also forms part of the descending auditory pathways. The IC receives both afferent input from several brainstem auditory nuclei (Beyerl 1978; Brunso-Bechtold et al. 1981; Druga and Syka 1984; Shneiderman et al. 1988) and is a well-established target of corticofugal projections from the auditory cortex (AC) (for reviews see Syka et al. 1988; Suga et al. 2000). The descending corticofugal system forms multiple feedback loops in the ascending auditory pathways. Cortical input to the IC is both divergent and convergent, with single cortical areas projecting to six or more collicular subdivisions (Winer et al. 1998). Neurons in layer V of the auditory cortex project to, among other auditory structures, the inferior colliculus (IC) (Kelly and Wong 1981; Saldana et al. 1996) with a tonotopic organization (Huffman and Henson 1990). Although corticocollicular fibers project bilaterally to the IC, the ipsilateral projection is much more extensive (Saldana et al. 1996; Druga et al. 1997). Winer and colleagues (1998, 2002) have demonstrated a significant projection from every cortical field to the IC in various mammalian species, including rat, cat, and squirrel monkey. The principal targets in the IC are the dorsal cortex, lateral nucleus, caudal cortex, and intercollicular tegmentum, with a sparse projection to the central nucleus. The heaviest AC projection terminates in the caudal half of the IC.

The physiological effects of corticofugal projections to the IC have been previously shown in bats (Sun et al. 1989; Yan and Suga 1996; Zhang and Suga 1997, 2000; Zhang et al. 1997; Jen et al. 1998; Yan and Suga 1998; Zhou and Jen 2000; Ma and Suga 2001a) and other mammals including rats (Syka and Popelar 1984; Syka et al. 1988), guinea pigs (Torterolo et al. 1998) and mice (Yan and Ehret 2001, 2002). These studies have demonstrated that corticofugal modulation of IC neurons can be excitatory and/or inhibitory. As in other auditory structures, sound frequency is systematically represented as a tonotopic map in the IC. Recent studies in bats and mice indicate that corticofugal projections play a key role in the organization and reorganization of this map. Focal electrical activation of the AC elicits frequency-specific changes in tonotopy, frequency tuning, sensitivity and response patterns in the IC mediated by corticofugal projections (Yan and Suga 1996, 1998; Zhang and Suga 1997, 2000; Jen et al. 1998; Zhou and Jen 2000; Yan and Ehret 2001, 2002).

While the fundamental importance of corticofugal modulation of IC processing of auditory information cannot be refuted, the functional role of corticofugal projections is poorly understood in animals with non-specialized auditory systems (Syka and Popelar 1984; Torterolo et al. 1998; Yan and Ehret 2001, 2002). Moreover, our understanding of the corticofugal pathways is limited by an incomplete picture of their functional influence within the three-dimensional (D) space of the IC. One of the recent technical advances that could assist in providing this information is the development of micromachined multichannel silicon probes. This involves the use of solid-state process technology to realize probes in which a precisely etched silicon substrate supports an array of thin-film conductors insulated above and below by deposited dielectrics. Openings in the dielectrics, produced using photolithography, form the recording sites, which permit recording from single or small groups of neurons on a highly selective basis. The fabrication process for microprobe structures have made possible great strides in the development and use of 1-D single-shank probes, 2-D planar probes and, more recently, 3-D arrays to study the processing of neural information (Najafi et al. 1985; Ji and Wise 1992; Hoogerwerf and Wise 1994; Chen et al. 1997).

Micromachined silicon probes now allow the realization of recording arrays having sites lithographically controlled with spacings as small as a few microns on supporting shanks 10–15 μm thick and less than 30 μm wide. Such probes have been used successfully by many physiologists to explore new aspects of neural systems in acute experimentation, recording neural responses to various stimuli simultaneously from a large number of neurons (Bragin et al. 1995; Harris et al. 2000), and there is growing interest and success in using these devices for chronic recording (Bragin et al. 2000; Mensinger et al. 2000). In the present study we have used these probes to systematically map the properties and spatial representation of corticofugal input in the IC of guinea pig with a high degree of spatial resolution.

## Materials and methods

Experiments were performed on healthy female, adult pigmented guinea pigs (Elm Hill Breeding Labs, Chelmsford, MA) with normal Preyer's reflexes, weighing 289–656 g. All procedures were performed in accordance with NIH guidelines for the care and use of laboratory animals (NIH publication No. 80-23) and guidelines provided by the Institutional Animal Care and Use Committee of the University of Michigan.

### Surgical preparation

The animals were anesthetized with a mixture of ketamine (Ketaset, 80 mg/kg, i.m.) and xylazine (Rompun, 4 mg/kg, i.m.) and held in a stereotaxic device (Kopf) with hollow ear bars for the delivery of sounds. Supplemental doses of ketamine (40 mg/kg) were administered every 60–90 min to maintain anesthetic levels throughout the experiment. Rectal temperature was monitored and maintained at 38°±0.5°C with a thermostatically controlled heating pad. The scalp overlying the dorsal skull was removed and two holes drilled in the skull to expose the right AC and right IC. The hole for the IC was sufficiently large to expose the midline blood vessels and the transverse sinus, located in the dura between the cerebellum and occipital cortex that overlies the IC. The dura mater was carefully removed to always expose the same A1 region (anterior auditory field according to Redies et al. 1989). To expose the IC, the dura over occipital cortex was removed. Care was taken to cut the dura as close as possible to the transverse sinus and midline blood vessels since these were used as landmarks for establishing the initial coordinates in the spatial mapping. The occipital cortex was aspirated to directly visualize the IC in many of the experiments, especially those involving the electrode with 32 recording sites (see below).

### Recording and stimulating electrodes

We systematically mapped neural activity in the IC using silicon substrate probes that allow for simultaneous recording at multiple neural sites. Two types of probes were used. They were fabricated by the Center for Neural Communication Technology in the University of Michigan Electrical Engineering and Computer Science Department. The first probe was a single shank device with 16 recording sites spaced at 100-μm intervals that provided a high spatial resolution in the dorsal-ventral plane. The second probe, which was specially designed and fabricated for this study, had 32 recording sites (Fig. 1). They were distributed across a four-shank array with eight recording sites spaced at 200-μm intervals on each shank. The four shanks, which were separated by 250 μm, provided high spatial resolution in the medial-lateral plane. The electrode for stimulating the AC was a concentric bipolar electrode having an outer pole 200 μm in diameter and a 50-μm stainless steel inner conductor.

### Neural recordings

Neural recordings were obtained with the silicon probes using headstages and amplifiers connected to a multi-channel data acquisition system capable of simultaneously recording up to 32 channels of single-unit data (Plexon, Dallas, TX). The system consists of a signal-input board which provides programmable gain, filtering (bandwidth 0.3–10 kHz) and analogue-to-digital (A/D) conversion. Responses of single units and unit clusters were

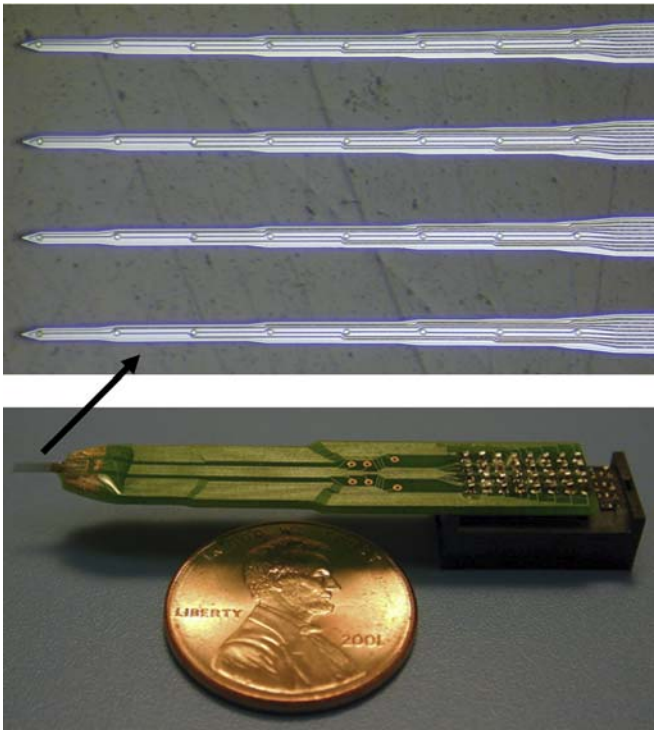


**Fig. 1** The four-shank, multichannel recording electrode used in this study. The recording sites are distributed across the four-shank array with eight recording sites spaced at 200-μm intervals. The four shanks are separated by 250-μm intervals to provide high spatial resolution in the medial-lateral plane

digitized with 12-bit resolution at 40 kHz on all channels simultaneously. Signals were then routed to multiple digital signal processor boards for computer-controlled spike waveform capture and sorting. The processor was controlled by a Pentium III 600 Mhz, with 768 MB RAM running under Windows NT, using a dual-monitor display. The system has a suite of software packages for real-time and off-line spike sorting (e.g., template matching and principle component analysis), spike-waveform tracking (Wave-Tracker software) and data analysis (Neuroexplorer software). Peri-stimulus time histograms (PSTHs) for all 16 or 32 recording sites were simultaneously displayed in real time and analyzed off-line to establish response properties of IC neurons to acoustic stimulation of the cochlea and electrical stimulation of the AC.

## Acoustic and electrical stimuli

Acoustic and electrical stimuli were digitally generated using Tucker-Davis Technology (TDT) System II/System III hardware and SigGen and Sigplay 3.2 software. The electrical stimulus consisted of biphasic, charge balanced rectangular pulses with a phase duration of 100 μsec presented at a rate of 3/sec. It was delivered to the stimulating electrode in the right AC via an optically isolated controlled-current stimulator (in-house fabricated) at current levels ranging from 0 to 100 μA. The digitally synthesized acoustic stimuli (100 ms duration, 5-ms rise-fall times) were delivered to the left ear at sound levels ranging from 0 to 60 dB SPL via a calibrated transducer (Beyer) coupled to the hollow ear bars. Monaural stimuli were used to characterize the excitatory responses that occur in response to contralateral acoustic stimulation.

## Experimental protocols

Experimental procedures were performed on 28 guinea pigs. In each experiment, the concentric bipolar stimulating electrode was advanced, perpendicularly to the brain surface, under visual control. It was always placed in the same A1 region of AC at a depth of approximately 700 μm. Either a 16- or 32-channel recording probe was then lowered across the tonotopic axis of the IC from a dorsal approach.

Our goal was to obtain detailed spatial maps of the responses in the IC produced by stimulation of auditory cortex. However, in the first 10 experiments the focus was to stimulate the AC at several current levels to characterize the types of responses and to establish their thresholds. Responses to acoustic stimuli at several frequencies and intensities were also recorded and the effects of electrical stimulation on responses to sound were assessed. These protocols took about 45 min to complete. Thus, it was not possible to record conveniently from more than 12–15 probe locations.

Detailed spatial maps were attempted in the remaining 18 animals. The IC was systematically sampled in the medial-lateral and rostral-caudal directions relative to the midline blood vessels and the transverse sinus, respectively. The initial puncture was made in the IC at a location that allowed us to place the electrode (or left shank of the four-shank array) as close as possible to midline and the cerebellum. Depending on the size and anatomical features of the animal this was usually 1.25–1.5 mm from midline and 1–1.75 mm in front of the transverse sinus. The probes were then systematically relocated at a more lateral position to establish a medial-lateral row of punctures. Single-shank probes were moved in either 200- or 500-μm steps, while the four-shank arrays were moved in 1.0-mm steps (relative to the left shank). This was then repeated at progressively more rostral locations with each row separated by 500 μm. With the 16-channel single-shank probes, the goal was to obtain six punctures in each row for at least seven rostral-caudal locations (a total of 42 punctures). The goal with the 32-channel four-shank electrodes was to obtain three punctures in each row for at least nine rostral-caudal locations (a total of 27 punctures).

With a large number of penetrations into the colliculus, it is possible that the probe could damage the tissue and/or its blood supply, which might influence the results. One advantage of the silicon probes is their small size (see above), producing less damage and enabling them to occupy a very small percentage of the total tissue volume (see Fig. 2). To reduce further the potential influence of injury, the rows of punctures were separated by 500 μm. Finally, in an attempt to avoid damage to the corticofugal projections entering the colliculus, sampling always proceeded from caudal to rostral.

Due to the number of probe placements, an abbreviated experimental protocol was used in the detailed mapping experiments. At each probe location, acoustic responses to three frequencies (2, 10 and 20 kHz) at 40 or 60 dB SPL and electrical responses at three current levels (usually 20, 60 and 100 μA) were recorded. This protocol took about 15 min to complete at each probe location, making it possible to record conveniently from 27 or 42 probe locations. Detailed spatial maps were obtained from seven animals (three with 32-channel probes) that comprise the bulk of the data for this paper.

## Histology

At the end of each of experiment, the animal was decapitated and the head immersed in 10% formaldehyde. The brain was removed, placed in 20% sucrose solution and then cryosectioned at 40 μm in the sagittal plane. The sections were mounted on slides and examined for evidence of recording electrode locations. Although evidence of electrode tracks could be seen with the thin silicon probes (Fig. 2, *top panel*) not all the tracks were commonly observed. Thus, to help identify electrode tracks, the recording probes in the mapping experiments were dipped in Fluorogold (2%). This was done once in a given experiment, for either the first, last or

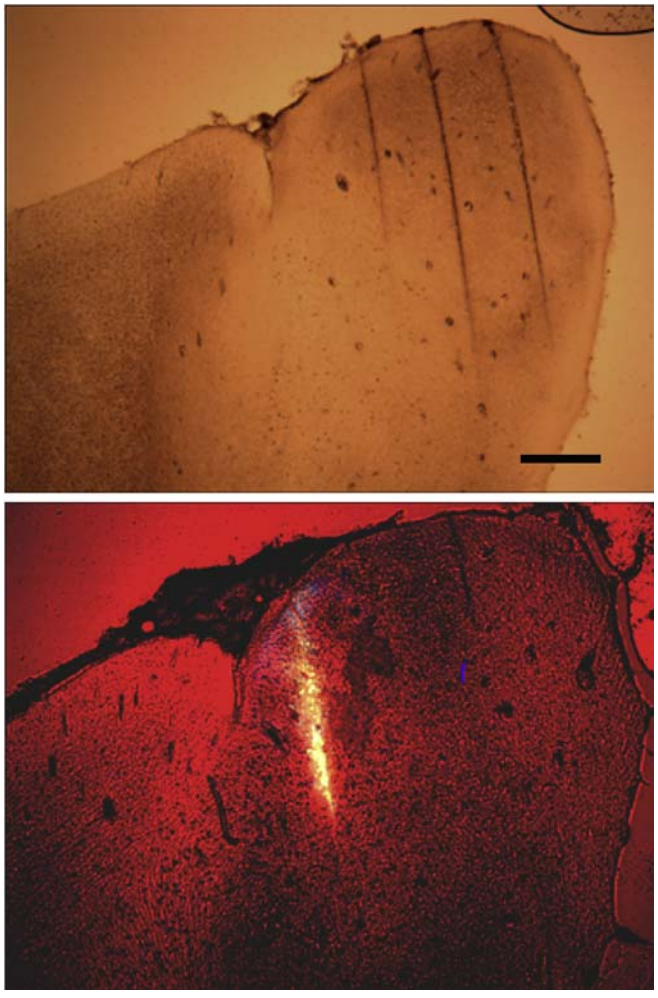

**Fig. 2** Photomicrographs of electrode tracks in the IC. The sections are unstained and were cut at a 40-µm thickness in the sagittal plane. Tracks can be seen as a result of three rostral caudal placements (*top panel*) separated by 500 µm. The most caudal track was measured to be 0.66 mm from the caudal edge of the IC (adjusted for 10% tissue shrinkage). Note that the probes produce less damage than a conventional glass pipette and occupy only a small percentage of the tissue volume. In the *bottom panel* the probe had been dipped in Fluorogold (2%). The fluorescent track was measured to be 2.6 mm from the caudal edge of the IC. This is at the rostral-caudal location of the data depicted in Fig. 10. Based on such measurements, the rostral-caudal locations of all puncture locations were expressed relative to the caudal edge of the IC. The location of the tracks combined with the coordinates of the spatial map from the surface landmarks enabled a histological 3-D reconstruction of the electrode locations. Scale marker = 500 µm

middle puncture in the grid of probe locations. An example of a labeled track seen under epifluorescence is shown in Fig. 2 (*bottom panel*). The location of the labeled tracks combined with the coordinates of the spatial map from the surface landmarks enabled a histological 3-D reconstruction of the electrode locations.

## Results

### Neural activity

Upon placement of a recording electrode at the desired depth in the IC, the quality of neural recordings varied across the array of recording sites. Typically, between 30 and 50% of the sites in each puncture had one or up to three spikes of different amplitude that could be discriminated into single units using conventional spike sorting algorithms such as principal component analysis (Fig. 3C, E, G). The remaining sites had multi-unit neural hash (Fig. 3B, D, F). Neural hash is defined as neural activity evoked by acoustic or electrical stimulation that does not have a sufficient signal-to-noise ratio to permit reliable spike sorting. Due to the large number of sampled sites using 16- and 32-channel electrodes, no attempt was made to discriminate single units either in real time or off-line. Thus, the response patterns depicted in these results are generated largely by multi-unit activity.

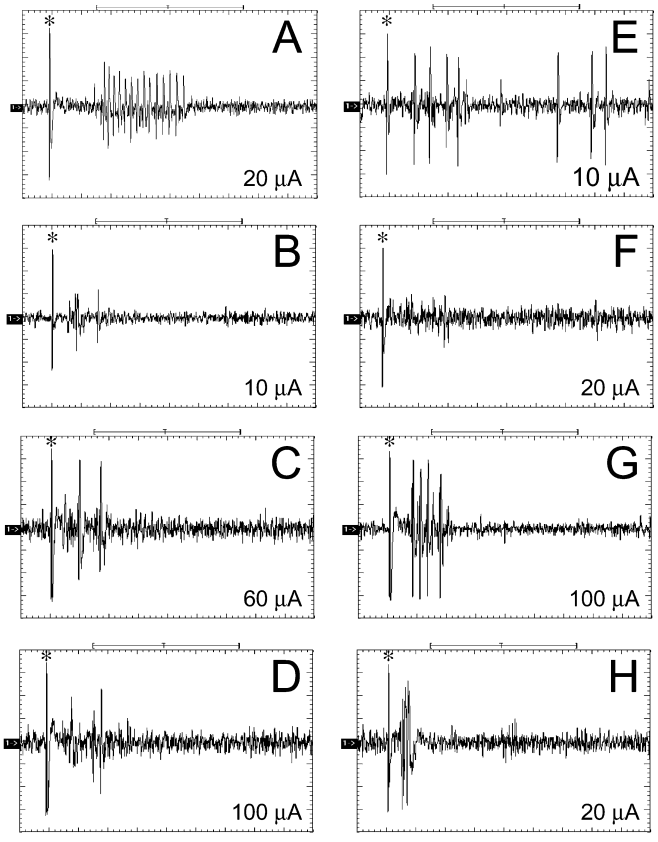


**Fig. 3A–H** Examples of multi-unit spike trains obtained from eight different channels of a multichannel recording probe. Easily discriminable unit spikes are seen in **A, C, E** and **G,** while multi-unit hash is seen in **B, D, F** and **H.** *Asterisks* indicate the stimulus artifact

## Responses to cortical electrical stimulation

Electrical stimulation of the ipsilateral AC produced excitatory responses in the IC with thresholds usually below 5–10 μA. First spike latencies in the 6–20 ms range predominated, although latencies from 3–5 ms were sometimes seen (see below). Broadly distributed unimodal spike patterns with modal latencies greater than 30 ms were occasionally seen. Peri-stimulus time histograms (PSTH) revealed the excitatory responses to cortical stimulation were mostly unimodal or occasionally bimodal with a wide range of spike distribution patterns (Fig. 4). The criterion for distinguishing unimodal and bimodal response patterns was spike distributions with two modal values separated by at least 5 ms. Figure 4 shows several PSTH response patterns obtained from the IC in response to electrical stimulation of the AC. The most common pattern was unimodal (see Fig. 4A, B, H), occurring at about 90% of the sites that exhibited a response, but the duration of this pattern showed considerable variability. The spike distribution patterns for both unimodal and bimodal responses (Fig. 4C, D, F, G) were categorized according to the duration of the response as short (<5 ms), medium (6–20 ms) and long (>21 ms) duration. The response durations and distribution patterns had a rather characteristic spatial distribution in the IC (see below). Occasionally, trimodal or complex responses occurred. These were defined as spike distribution patterns with more than two modal values each separated by at least 5 ms. In Fig. 4D the response pattern was classified as bimodal although it was borderline for meeting the criterion for trimodal. The trimodal (complex) patterns were usually seen only at higher current levels (>60 μA) and it is not clear how many of these were a consequence of the multi-unit recordings.

The spike distribution patterns and their latencies and durations were quantified in three experiments using 32-channel recording probes. In two of the experiments, data were obtained from 27 punctures while 26 punctures were made in the third experiment. This resulted in a total of 2,560 recording sites of which 1,183 (46%) exhibited an excitatory response to stimulation of the AC at 100 μA. An analysis of the spike distribution patterns revealed that 1,089 (92%) were unimodal, 87 (7%) were bimodal and 7 (<1%) were trimodal/complex. Twenty-two percent of first spike latencies (266) were categorized as having a short latency (<5 ms), 914 (77%) were in the medium category (6–20 ms) and only 3 (<1%) had a long latency (>21 ms). In terms of response duration, 19% (255) of the responses were categorized as short, 790 (67%) had a medium duration and 168 (14%) had a long duration.

In three of the initial experiments (22 punctures, 544 recording sites), responses were obtained at current levels ranging from 0–100 μA in 5–10 μA steps. This resulted in excitatory input-output functions that were predominantly monotonic, although some were non-monotonic. The excitation was frequently followed by suppression of spontaneous activity that lasted for 25–150 ms, more commonly at higher levels of current. Predominantly

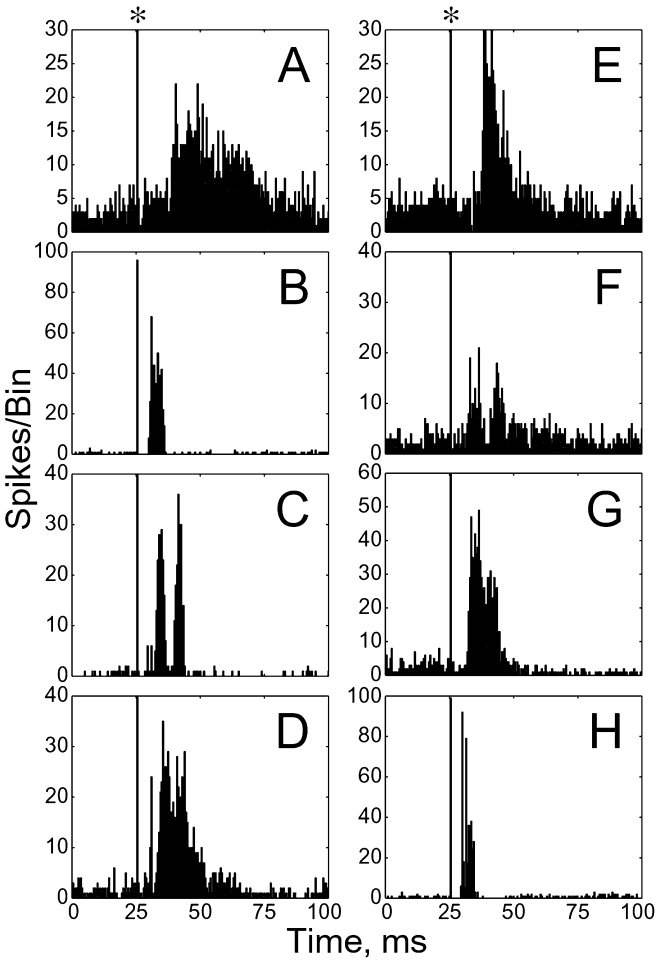


**Fig. 4A–H** Peri-stimulus time histograms (PSTHs) from IC neurons obtained in response to 100 presentations of a bipolar electrical stimulus presented to the auditory cortex. Uni- and bimodal excitatory responses are shown. These PSTHs were compiled from the unit responses shown in Fig. 3. The *asterisk* at the top of each column indicates the stimulus artifact. The data were collected in 0.5-ms time bins

inhibitory responses to electrical stimulation sometimes occurred (Fig. 5). Since the corticocollicular projections appear to use an excitatory amino acid as their transmitter (Feliciano and Potashner 1995), this suppression suggests disynaptic mechanisms of corticocollicular inhibition.

In a small number of experiments (n=4), the effect of electrical stimulation on responses to acoustic stimulation was assessed. Suppression of acoustic responses was often observed with the degree of suppression depending on the level of both the acoustic stimulus and the cortical stimulation. In a few instances the suppression of acoustic responses occurred even though there was little or no response to electrical stimulation, suggesting a form of spatial-temporal integration (Fig. 6). The results depicted in Fig. 6 show the most dramatic example of this effect with the adapted portion of the response to acoustic stimulation suppressed 56% by electrical stimulation (Fig. 6B), which had no effect on spontaneous activity when presented alone (Fig. 6C). This effect was quantified using 94 sites in the four experiments that met the criteria

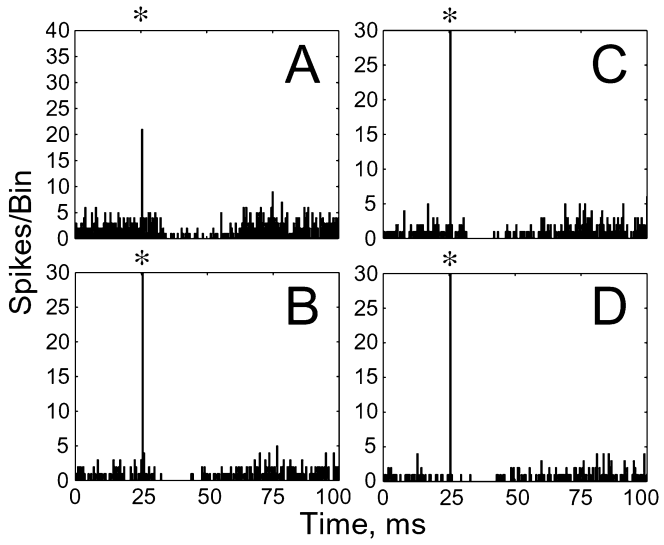


**Fig. 5A–D** Peri-stimulus time histograms (PSTHs) from IC neurons obtained in response to 100 presentations of a bipolar electrical stimulus presented to the auditory cortex. Although there is no clear excitatory response to the electrical stimulus, the spontaneous activity is clearly suppressed with suppression lasting for 40–60 ms. *Asterisks* indicate the stimulus artifact, which occurs at 25 ms in this and all subsequent figures. Current levels were 60 μA (**A** and **C**) and 100 μA (**B** and **D**). The data were collected in 0.5-ms time bins

of having a primary-like response lasting the duration of the acoustic stimulus (100 ms) and no apparent response to electrical stimulation at the current level studied. Spike counts were determined for the 50 to 100-ms segment of the responses to the tone with and without the electrical stimulus. Of the 94 sites, 59 exhibited suppression produced by the electrical stimulus, with 35 having a suppression of at least 10%. Of these 35, seven exhibited suppression greater than 20% with four displaying suppressions of 40, 44, 55 and 56%. It should be noted that if the position of the stimulus artifact for the electrical stimulation in Fig. 6B is marked on Fig. 6A, it can be seen that the form of the histogram in Fig. 6B with electrical stimulation changes before the stimulus occurs. In Fig. 6B the spike count for the 0 to 20-ms segment before the artifact is actually reduced 16%. Of the 35 sites that showed greater than 10% suppression of the adapted portion of the response to the tone, 24 sites exhibited suppression of the 0 to 20-ms segment, with 13 of these being greater than 10%.

## Spatial representation of corticofugal input in the IC

The different types of responses to cortical stimulation exhibited a characteristic distribution within the three-dimensional space of the IC. Figure 7 depicts several features of this distribution. The results were obtained with a 16-channel single-shank electrode that was placed at different locations lateral to the midline blood vessels to establish a row of punctures that was 1.9 mm rostral to the transverse sinus. The occipital cortex over the IC was intact in this experiment. The tip of the recording electrode was lowered to a depth of 4.5 mm at the medial-lateral locations indicated at the top of each column of peri-stimulus time histograms. The histograms in each column were obtained simultaneously to a current of 100 μA applied to the AC and depict increasing depth in the IC. In the two most medial punctures (1.5 and 1.7 mm from midline) predominantly unimodal and bimodal responses to cortical stimulation are strongest at the shallower recording sites. This area in the upper left of Fig. 7 was shown histologically to correspond to the dorsomedial region of the IC. Across experiments, in the most medial punctures (1.25–1.5 mm from midline) the responses tended to occur deeper and be a little more robust than in slightly more lateral punctures (1.5–1.75 mm from midline). The results depicted at 1.7 mm from midline in Fig. 7 show there is an area which has little if any excitatory response to electrical stimulation of AC. The deeper regions at 1.5 and 1.7 mm from midline correspond histologically to the central nucleus of the IC. In this animal, at 1.9 mm from midline the responses to cortical

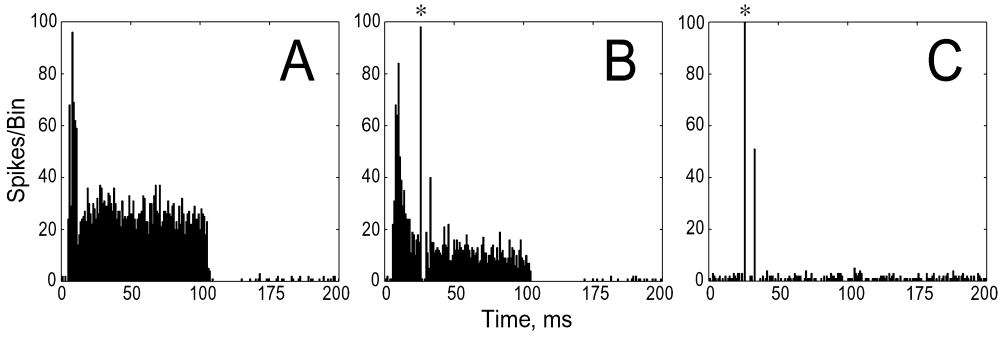


**Fig. 6A–C** Peri-stimulus time histograms (PSTHs) from IC neurons obtained in response to 100 presentations of a 100 ms, CF toneburst (10 kHz) presented alone (**A**) and with the addition of a bipolar electrical pulse applied to the auditory cortex (**B**). The onset of the electrical stimulus is indicated by the *asterisk* and is delayed 25 ms from the onset of the tone. In **B**, the electrical stimulus depresses steady state/adapted activity evoked by the tone, and in **C**, the electrical stimulus presented without the acoustic stimulus has no effect. These responses were obtained from animal ICes021502 at a location 1.4 mm rostral to the caudal edge of the IC and 1.5 mm from midline. This area responded robustly with primary-like responses to toneburst stimulation, but did not respond to electrical stimulation of AC alone. The *asterisks* indicate the stimulus artifact. The data were collected in 1.0-ms time bins

stimulation are more unimodal with depth in the IC and are also shorter in duration. Anatomically, this seemed to correspond to a transition zone between the central nucleus and the external cortex. Further lateral in the external cortex, as seen in *column 4* of Fig. 7, the responses are longer in duration. These were consistent findings across all the mapping experiments.

Although there was some variability between animals (due to differences in the anatomical landmarks used to establish the puncture coordinates), there was always an area largely devoid of excitatory responses to cortical stimulation in the caudal and medial region of the IC that occurred 1.5–2.25 mm from midline and 1.5–2.5 mm rostral to the caudal edge of the IC. However, as depicted in Fig. 8, this was an area that exhibited the most primary-like responses to acoustic stimulation and a clear tonotopic organization. In this figure, the results were obtained at one location with the electrode placed 1.8 mm rostral to the caudal edge of the IC, 1.5 mm from midline and at a depth of 5.0 mm through the intact occipital cortex. Each column of peri-stimulus time histograms was obtained simultaneously to acoustic stimulation at the indicated frequencies or electrical stimulation of auditory cortex at 100 μA. Although all three acoustic stimuli were presented at 60 dB SPL, the responses are tonotopically distributed across the array of recording sites with areas of maximal excitation located progressively deeper with increasing frequency. There was virtually no excitatory response to electrical stimulation. However, in this and other animals, this region of the IC often exhibited suppression of spontaneous and sound-evoked activity by electrical stimulation of the AC. Our sample of sites showing suppression of acoustic responses is limited (see above) and we have made no attempt to quantify the number of recording sites showing suppression of spontaneous activity (Fig. 5). However, the suppression of spontaneous activity appeared to be less common than reported by other investigators (Syka and Popelar 1984; Torterolo et al. 1998), perhaps due to the multi-unit recordings masking the effect in the present study.

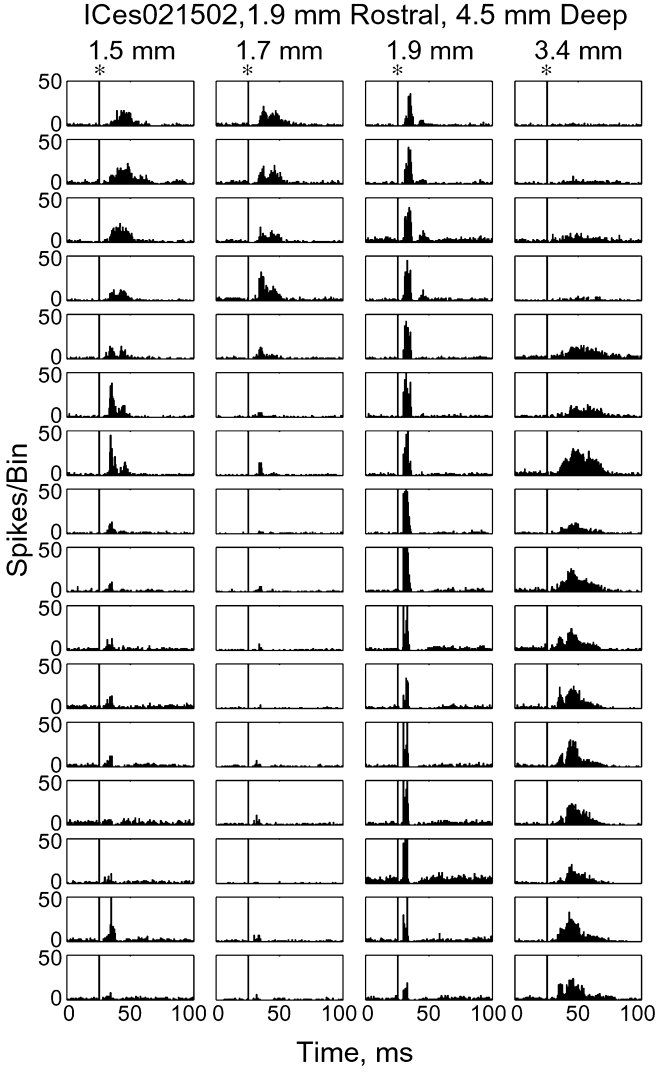


**Fig. 7** Peri-stimulus time histograms (PSTHs) from IC neurons obtained in response to 100 presentations of a bipolar electrical stimulus presented to the auditory cortex. Each column shows the responses at 16 sites of a 16-channel probe placed at locations, 1.5, 1.7, 1.9 and 3.4 mm, respectively, from the midline and at 1.9 mm rostral to the caudal edge of the IC. Depth increases towards the bottom of the figure, with the tip of probe placed at a depth of 4.5 mm. The depth in this figure is relative to the surface of the occipital cortex since the cortex was not aspirated in this experiment. The more medial channels show stronger responses at shallower depths, while more lateral locations show stronger responses at deeper locations. Note the limited responsiveness in the 1.7-mm area to electrical stimulation. The *asterisk* at the top of each column indicates the stimulus artifact. The data were collected in 0.5-ms time bins

Results comparable to those depicted in Fig. 7 are shown in Fig. 9 but in this case they were obtained using the 32-channel four-shank electrode. The electrode was initially placed with the left-most shank 1.25 mm from midline and the tip lowered in the IC to a depth of 2.75 mm (the overlying cortex had been aspirated to visualize the surface of the IC). After recording at this location, the probe was raised, moved 1.0 mm lateral and the tip lowered again to a depth of 2.75 mm. The procedure was again repeated at 3.25 mm from midline. Thus, the columns of PSTHs depict responses separated by 250 μm and ranging in distance from midline from 1.25 to 4.0 mm. It can be seen that in medial locations there are many sites that fail to respond with excitation to electrical stimulation of the AC at 100 μA. This again is an area that was tonotopically organized and exhibited a high percentage of primary-like response patterns to tonal stimulation. Moving laterally, the responses are more robust, with the most lateral responses being of longer duration than those seen at more central locations in the matrix of responses. The more lateral responses also exhibit a higher number of bimodal response patterns. The responses to acoustic stimulation at these locations tended to be less primary-like and less tonotopically organized. A somewhat similar pattern is seen at locations that are 500 μm more rostral (Fig. 10) but here there are greater numbers of medial sites that respond to the electrical stimulus. This is at the rostral-caudal location depicted by the fluorescent track in Fig. 2 (*bottom panel*). Moving

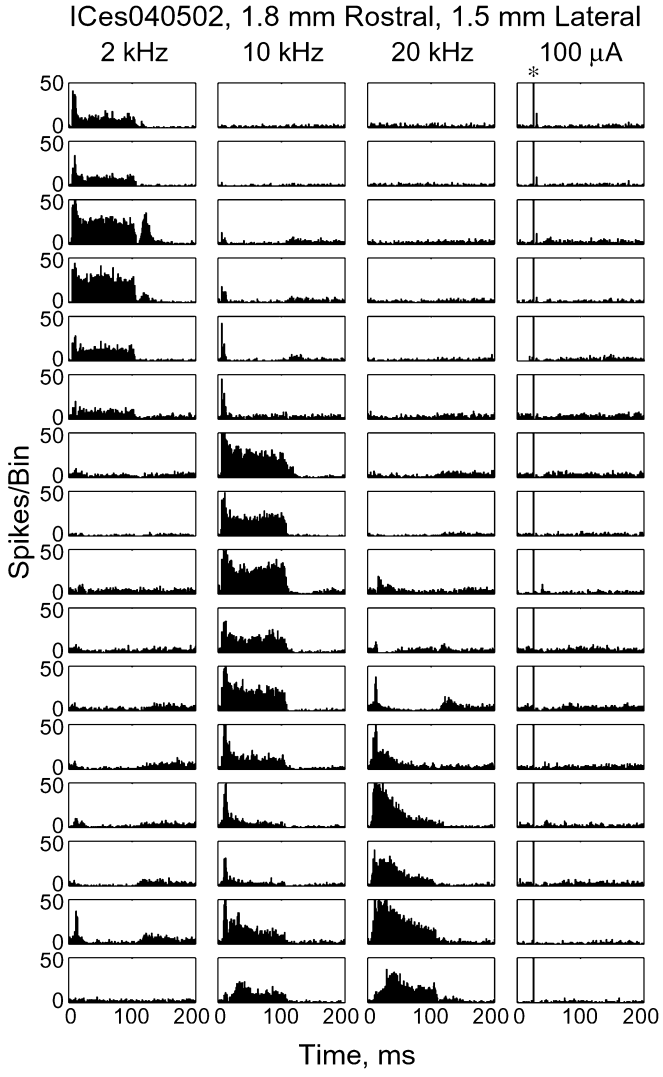


**Fig. 8** Peri-stimulus time histograms (PSTHs) from IC neurons at one location (1.75 mm rostral, 1.5 mm lateral), obtained in response to 100 presentations of a toneburst. Each column shows the response of 16 sites to a different frequency of stimulation. Depth increases towards the bottom of the figure, with the tip of the probe placed at a depth of 5.0 mm through the intact occipital cortex. Responses to lower frequencies are restricted to shallower locations, and responses to higher frequencies are restricted to deeper locations, in keeping with the tonotopicity of this structure. Note that the same location showed limited responsiveness to electrical stimulation of the AC (*right column*). The *asterisk* at the top of the right column indicates the stimulus artifact. The data were collected in 1.0-ms time bins

further forward (Fig. 11), weaker responses with higher thresholds tend to be distributed centrally in the matrix while more robust responses are located at deeper and more lateral locations. The histology clearly revealed this row of punctures was located in the superior colliculus (SC). At these more rostral locations, the responses are generally longer in duration and less robust, occurring as far forward as 5.0–5.5 mm in front of the caudal edge of the IC.

## Discussion

### Advantages of the use of micromachined silicon probes for IC mapping

Typically, when recording single units in the brain, an electrode is moved to sample multiple neurons. Thus, different neurons are assessed at different times. The critical element provided by silicon probes is their ability to be placed into a 3-D volume of tissue and sample multiple neurons simultaneously. This provides the ability to determine how an array of neurons react to a stimulus over a short period of time, e.g., to image the microstructure of spatial and temporal information across a population of cells.

The use of multicontact micromachined silicon probes for systematic mapping of the IC has several advantages. First, the very small size of the probe allows for multiple punctures with minimal tissue damage. Another interesting property of these probes is the very good geometry of the recording sites. Third, the large number of recording sites (32) and the resulting speed of data collection allow the analysis of a very large number of active neural units in a physiological stable animal. Consequently, the use of multicontact thin-film silicon probes offers for the first time a highly convenient way to spatially map the response characteristics of neurons in the central nervous system. For example, to record the same amount of information in one experiment in which we made 27 punctures with the 32-channel, four-shank probe would have taken approximately 9 days using conventional electrode techniques.

Recording bias is a common concern when using any type of electrode to sample the nervous system. Thus, it is not clear how many “no-response” or “little-response” panels (locations) in Figs. 7, 8, 9, 10 and 11 just show artifacts because the electrode tip did not pick up the response of a nearby unit. Since we systematically moved the electrodes most often in 500-μm steps, it is entirely possible that the spatial distributions of responsiveness do not depict the entire picture. However, due to the large number of punctures, we believe the responses and their distributions are a valid sample of activity. Moreover, since there is anatomical variability in the landmarks we used to establish initial coordinates for the mapping, it is less likely that we sampled the same areas in each experiment, thus lessening the sampling bias.

### Characteristics of the effect of cortical stimulation on IC neurons

Our results show that in guinea pig the cortigofugal modulation on IC neurons is highly heterogeneous: excitatory, inhibitory, or both kinds of responses are observed with diverse latencies, spike distribution patterns, and thresholds to electrical stimulation. These results confirm and extend the findings of Torterolo et al. (1998) in the guinea pig IC. They are also consistent

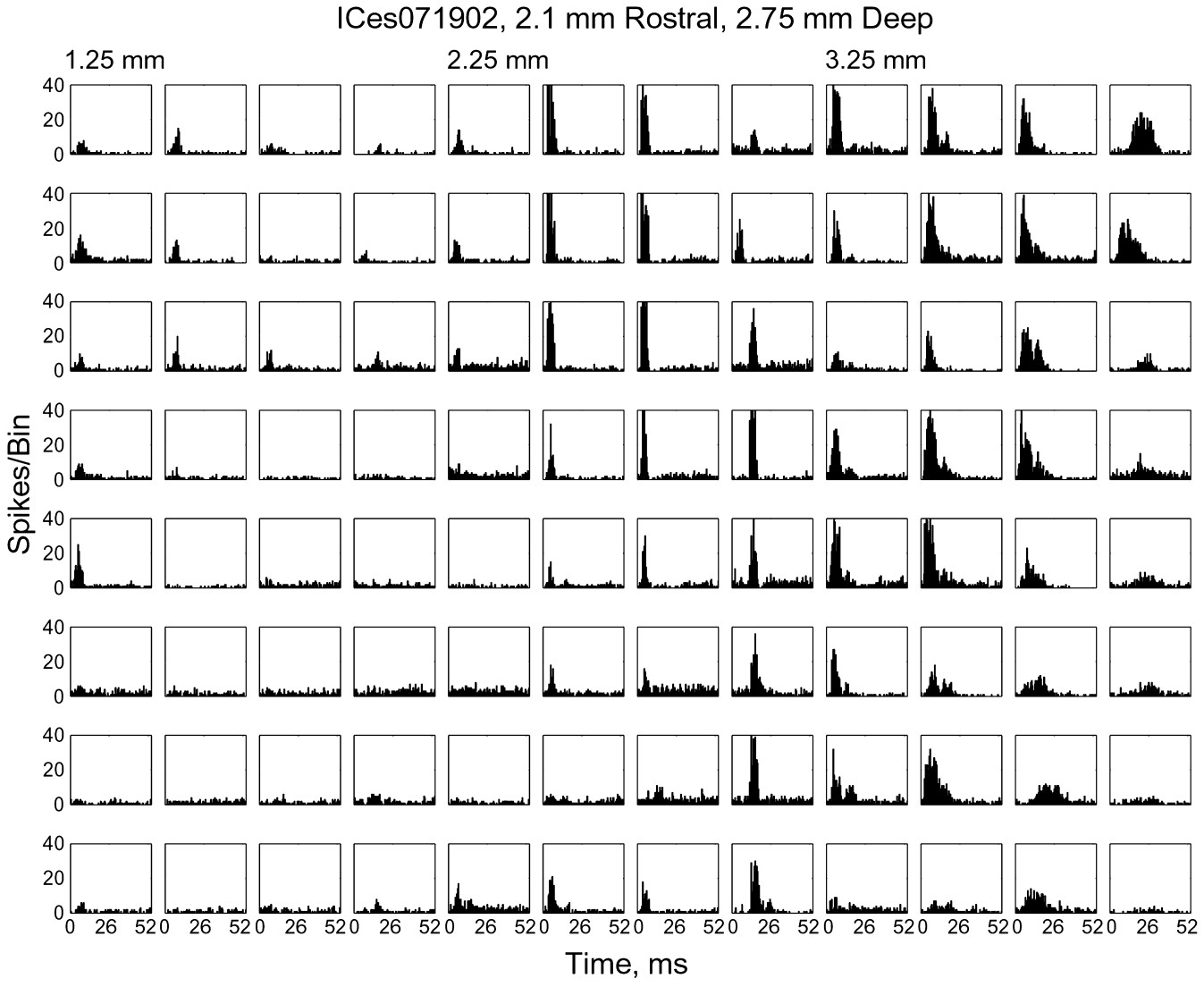


**Fig. 9** Peri-stimulus time histograms (PSTHs) from IC neurons at three locations (1.25, 2.25 and 3.35 mm from midline) obtained in response to 100 presentations of a 100-μA electrical stimulus applied to AC. Each group of four columns (3) represents the responses of neurons on the 32-channel, four-shank electrode. Each column then depicts the responses of neurons separated by 250 μm in the medial-lateral plane and 100 μm in the dorsal-ventral plane. The electrode was moved in the medial direction twice to obtain the lateral-medial map depicted here. Histology revealed that this row of punctures was obtained at a rostral-caudal location that was 2.1 mm in front of the caudal edge of the IC. Depth increases towards the bottom of the figure, with the tip of the probe placed at a depth of 2.75 mm from the surface of the IC (cortex aspirated). Note the lack of responsiveness in many medial locations and the more robust responses in the more lateral locations. The abscissa in this and all subsequent figures depicts time for 52 ms after the stimulus artifact. The abscissas were shifted to exclude the stimulus artifact for the sake of clarity with the large number of PSTHs presented. Thus, time zero corresponds to the time of the stimulus artifact. The data were collected in 0.5-ms time bins

with the findings of Syka and Popelar (1984) in the rat. Suppression of spontaneous activity by electrical stimulation of the AC in at least a few IC neurons has been a common finding. This could occur via a disynaptic mechanism involving inhibitory GABAergic neurons in the IC (Oliver et al. 1994) and their innervation by excitatory glutamatergic descending fibers (Feliciano and Potashner 1995). The suppression of sound-evoked responses in the IC by electrical stimulation of the AC has generally been reported to occur in conjunction with a suppression of spontaneous activity. However, we observed that suppression of acoustic responses in the IC occurred at a small number of sites (35) in the absence of any discernable effects of cortical electrical stimulation on spontaneous activity. This is interesting and could be explained by spatial-temporal integration, perhaps involving a neural network. Alternatively, it could be due to the multi-unit recordings masking the suppression of spontaneous activity. In this regard, it is of interest that Torterolo et al. (1998) reported suppression of acoustically evoked responses but only in neurons that exhibited little if any spontaneous activity. Additional mapping studies using spike sorting techniques to resolve single units are needed to answer this question.

In addition to the suppression of the adapted portion of the acoustic response, electrical stimulation suppressed the

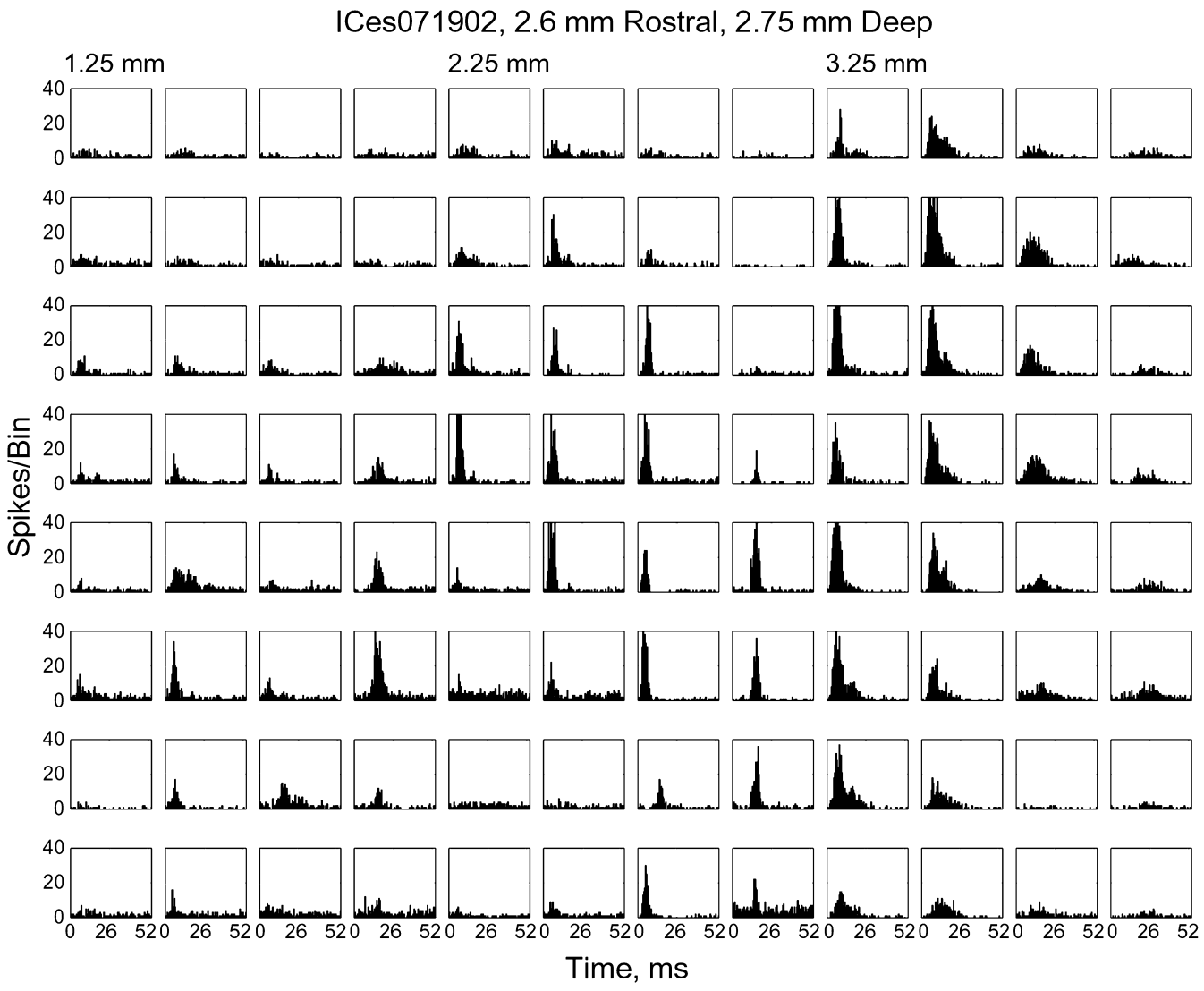


**Fig. 10** Peri-stimulus time histograms (PSTHs) from IC neurons at three locations (1.25, 2.25 and 3.35 mm from midline), obtained in response to 100 presentations of a 100-μA electrical stimulus applied to AC. These locations are 500 μm more rostral to the locations represented in Fig. 7 and at a location histologically confirmed to be 2.6 mm in front of the caudal edge of the IC (see Fig. 2). Each group of four columns (3) represents the responses of neurons on the 32-channel, four-shank electrode. Each column then depicts the responses of neurons separated by 250 μm in the medial-lateral plane and 100 μm in the dorsal-ventral plane. The electrode was moved in the medial direction twice to obtain the lateral-medial map depicted here. Depth increases towards the bottom of the figure, with the tip of the probe placed at a depth of 2.75 mm from the surface of the IC (cortex aspirated). In this more rostral location, more medial sites respond to the electrical stimulus. Note the lack of responsiveness in many medial locations and the more robust responses in the more lateral locations. Time zero as described in Fig. 9. The data were collected in 0.5-ms time bins

portion of the response that occurred before the electrical stimulus (Fig. 6). This too could be explained by spatial-temporal integration involving a neural network. With a stimulus rate of 3/sec it is conceivable that the effect of the electrical stimulus on synaptic potentials in a polysynaptic network is sufficiently sustained that it affects the beginning of the subsequent response in the series. Experiments in which the interstimulus interval is varied would help to address this question.

Our findings are consistent with the corticofugal modulation studies by Yan and Ehret (2001, 2002) in mouse and also consistent with the "multiparametric" characteristics of corticofugal modulation observed in mammals with a highly specialized auditory system. For example, in bats corticofugal modulation affects 1) frequency (Zhang and Suga 1997, 2000; Yan and Suga 1998; Ma and Suga 2001a; Gao and Suga 1998, 2000); 2) duration (Ma and Suga 2001b); and 3) parameters characterizing behaviorally relevant sounds (Yan and Suga 1996, 1999). This apparent complexity of the parameters on which descending pathways act can easily be understood if the complex acoustical parameters of sounds used by animals are considered. If corticofugal modulation were limited to only one sound parameter (for example frequency or duration), the adjustment of the central auditory system for auditory signal processing would only be partial.

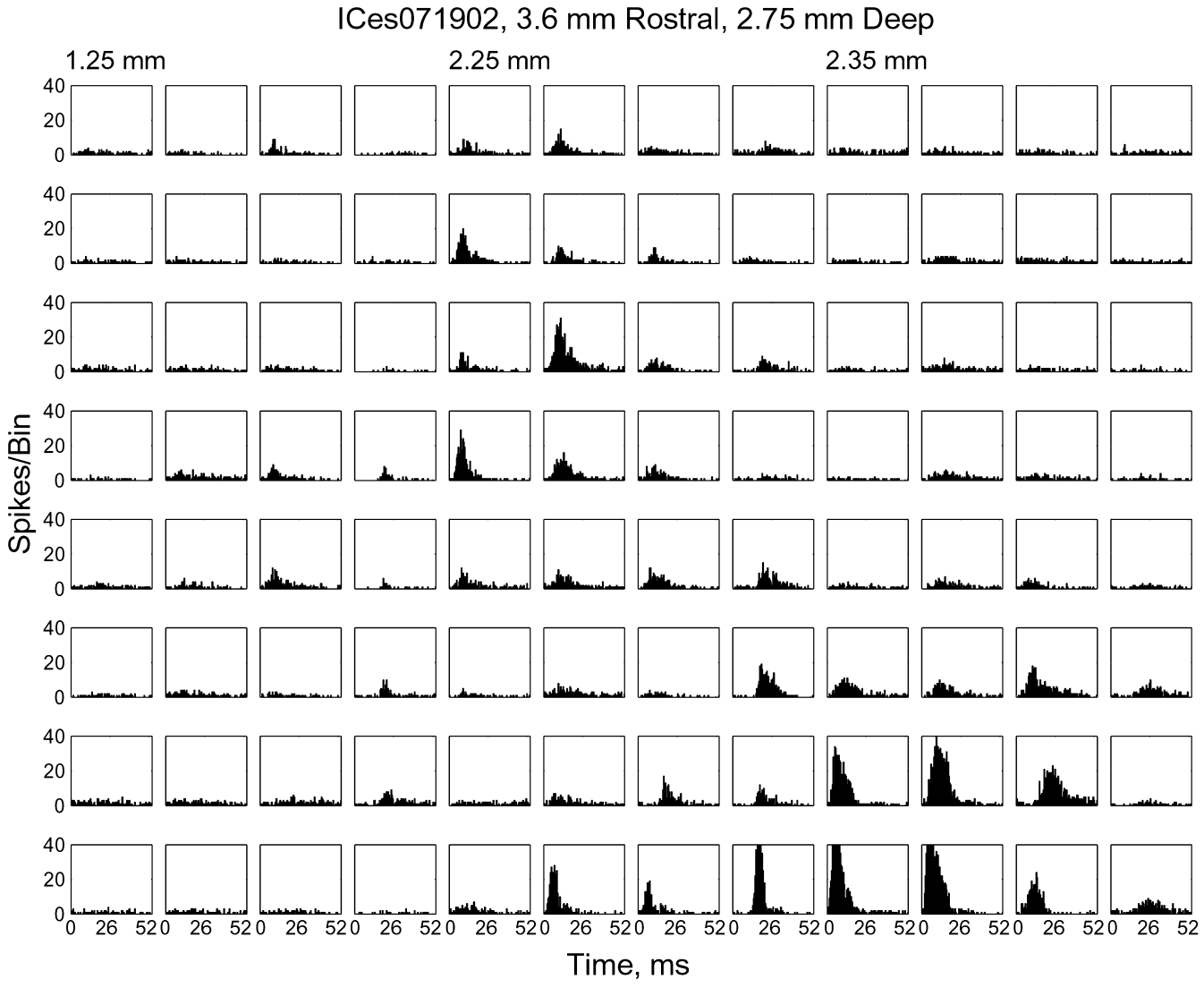


**Fig. 11** Peri-stimulus time histograms (PSTHs) from superior colliculus (SC) neurons at three locations (1.25, 2.25 and 3.35 mm from midline) obtained in response to 100 presentations of a 100-μA electrical stimulus applied to AC. These locations are 1.0 mm more rostral to the locations represented in Fig. 10 and are histologically confirmed to be in the SC. Each group of four columns (3) represents the responses of neurons on the 32-channel, four-shank electrode. Each column then depicts the responses of neurons separated by 250 μm in the medial-lateral plane and 100 μm in the dorsal-ventral plane. The electrode was moved in the medial direction twice to obtain the lateral-medial map depicted here. Depth increases towards the bottom of the figure, with the tip of the probe placed at a depth of 2.75 mm from the surface of the IC (cortex aspirated). In this more rostral location, more medial sites respond to the electrical stimulus. Note that at this location responsiveness is seen centrally in the matrix, but is less robust than the responses that appear deeper in the more lateral locations. Time zero as described in Fig. 9. The data were collected in 0.5-ms time bins

## Spatial representation of corticofugal input in the IC

Anatomical studies have demonstrated the descending pathways from the AC to the IC in cat (Andersen et al. 1980) and other species, including monkey (Fitzpatrick and Imig 1978) and rat (Saldana et al. 1996). Cortical input to the IC is both divergent and convergent, with single cortical areas projecting to six or more collicular subdivisions (Winer et al. 1998). The principal targets in the IC are the dorsal cortex, lateral nucleus, caudal cortex, and intercollicular tegmentum, with a more sparse projection to the central nucleus. The heaviest AC projection terminates in the caudal half of the IC. These anatomical findings provide the substrate to explain the changing spatial distribution of responses at different locations in the IC we observed in the present study. Responsiveness to cortical stimulation was more robust for punctures in the caudal half of the spatial map and became weaker in more rostral locations. There was an area in the dorsomedial region of the caudal half of the IC that exhibited a number of responsive sites. The more lateral punctures contained the most robust responses, with the duration of the responses being longer at more lateral locations. Rostrally, in addition to being weaker, the responses tended to be located at more central and ventrolateral regions, especially as the punctures moved into the SC. In future studies

it will be of interest to determine if there are differences in the influence of cortical stimulation on the processing of acoustic information in these different areas and the interactions between visual and auditory pathways.

There is little information in the literature on the spatial distribution of cortically evoked response properties in the IC. Syka and Popelar (1984) reported that responses in the rat IC to cortical stimulation were found mainly in the dorsomedial part of the central nucleus (dorsal cortex) and in the caudal and dorsal regions of the IC. Our findings are consistent with this observation. Syka and Popelar (1984) also reported that neurons in the external cortex of the IC were mostly inhibited by AC stimulation. In contrast, however, we found that at lateral locations, which correspond to the external cortex, the responses were mostly excitatory and robust. Inhibition was observed at more medial and caudal locations in the IC. Additional studies are needed to resolve this discrepancy. However, our findings are consistent with morphological data showing that cortical input to the dorsal cortex and lateral nucleus of IC is monosynaptic, while axons ending in the central nucleus have two projection modes: monosynaptic *via* thin corticocollicular fibers and polysynaptic *via* association pathways within the inferior colliculus (Winer et al. 2002).

## Functional interpretation of the role of descending pathways

It is now well established that corticofugal pathways play a significant role in central auditory plasticity being involved in the organization and reorganization of frequency maps under different conditions. Corticofugal feedback may play an important role in the manifestation of tinnitus (Langner and Wallhauser-Franke 1999). Tinnitus has been shown to be accompanied by a reorganization of tonotopy (Muhlnickel et al. 1998). Corticofugal modulation may also play a significant role in learning-induced plasticity in the IC (Gao and Suga 1998, 2000; Sakai and Suga 2001)

As occurs in other sensory modalities (particularly the visual and somatosensory systems), deafferentation of the peripheral auditory system leads to significant plastic changes in central pathways (Bledsoe et al. 1995; Klinke et al. 1999; Kral et al. 2002; Syka 2002 for review). Clearly, deafness induces plastic changes in the electrophysiological responsiveness of neurons in the ascending central auditory system, including the IC (Bledsoe et al. 1995). In most cases of deafness-induced plasticity, a common denominator is a deterioration of inhibition in the subcortical auditory nuclei and the auditory cortex. It is not clear how these changes induced by deafness would influence and perhaps alter the mechanisms of plasiticity associated with corticofugal pathways.

Changes in the structure and function of the central auditory system would be expected to produce a reorganization of the projection maps in the auditory cortex. Because of the projections of IC to the medial geniculate body whose closest auditory affiliations are with cortical regions involved in higher order auditory perception, the cortico-collicular system may link brainstem and colliculo-thalamic circuits to coordinate perceptual aspects of hearing (Winer et al. 1998). However, in addition to the processes that are altered by decreased or lost receptor function in the ascending pathway, little is known regarding deafness-induced changes in corticofugal and other descending pathways. In light of the aging world population and the increasing amount of noise in our modern world, the study of the neural mechanisms underlying the plasticity of the central auditory system is of high priority. Mapping the exact physiological location in the IC that corresponds to specific corticofugal projection patterns is thus an essential prerequisite to analyze and quantify the changes that occur with deafferentation.

## Future directions

Multichannel silicon probes offer a convenient and reliable means to sample from large numbers of neurons with a high degree of spatial resolution. In future directions it would be of interest to examine corticofugal influences on acoustically evoked responses and frequency maps within the three-dimensional space of the IC. By incorporating stimulation sites into IC probes, it should be possible to examine internuclear interactions and modulation of corticocollicular projections. These devices also open the door to examine integration in the IC with auditory and non-auditory corticofugal projections as well as ascending projections to the IC.

**Acknowledgements** We are grateful to Sufen Shang for skilled technical assistance and data processing and to Chris Ellinger for invaluable electronic support. The Center for Neural Communication Technology (CNCT) in the Department of Electrical Engineering and Computer Science supplied the multichannel electrodes used in this study. This work was supported by National Institutes of Health grants NIH-NIDCD DC00078, NIH-NIBIB EB00308 and NIH-NCRR RR09754.

## References

Aitkin LM (1986) The auditory midbrain. Structure and function in the central auditory pathway. Humana Press, Clifton, NJ

Andersen RA, Snyder RL, Merzenich MM (1980) The topographic organization of corticocollicular projections from physiologically identified loci in the AI, AII and anterior auditory cortical fields of the cat. J Comp Neurol 191:479–494

Beyerl BD (1978) Afferent projections to the central nucleus of the inferior colliculus in the rat. Brain Res 145:209–223

Bledsoe SC Jr, Nagase S, Miller JM, Altschuler RA (1995) Deafness-induced plasticity in the mature central auditory system. Neuroreport 7:225–229

Bragin A, Jando G, Nadasdy Z, Hetke J, Wise K, Buzsaki G (1995) Gamma (40Hz-100 Hz) oscillation in the hippocampus of the behaving rat. J Neurosci 15:47–60

Bragin A, Hetke J, Wilson CL, Anderson DJ, Engel Jr J, Buzsaki G (2000) Multiple site silicon-based probes for chronic recordings in freely moving rats: implantation, recording and histological verification. J Neurosci Meth 98:77–82

Brunso-Bechtold JK, Thompson GC, Masterton RB (1981) HRP study of the organization of auditory afferents ascending to central nucleus of inferior colliculus in cat. J Comp Neurol 197:705–722

Chen J, Wise KD, Hetke JF, Bledsoe SC Jr (1997) A multichannel neural probe for selective chemical delivery at the cellular level. IEEE Trans Biomed Eng 44:760–769

Druga R, Syka J (1984) Ascending and descending projections to the inferior colliculus in the rat. Physiol Bohemoslov 33:31–42

Druga R, Syka J, Rajkowska G (1997) Projections of auditory cortex onto the inferior colliculus in the rat. Physiol Res 46:215–222

Feliciano M, Potashner SJ (1995) Evidence for a glutamatergic pathway from the guinea pig auditory cortex to the inferior colliculus. J Neurochem 65:1348–1357

Fitzpatrick KA, Imig TA (1978) Projections of auditory cortex upon the thalamus and midbrain in the owl monkey. J Comp Neurol 177:537–556

Gao E, Suga N (1998) Experience-dependent corticofugal adjustment of midbrain frequency map in bat auditory system. Proc Natl Acad Sci USA 95:12663–12670

Gao E, Suga N (2000) Experience-dependent plasticity in the auditory cortex and the inferior colliculus of bats: role of the corticofugal system. Proc Natl Acad Sci USA 97:8081–8086

Harris KD, Henze DA, Csicsvari J, Hirase H, Buzaki G (2000) Accuracy of tetrode spike separation as determined by simultaneous intracellular and extracellular measurements. J Neurophysiol 84:401–414

Hoogerwerf AC, Wise KD (1994) A three-dimensional microelectrode array for chronic neural recording. IEEE Trans Biomed Engr 41:1136–1146

Huffman RF, Henson OW Jr (1990) The descending auditory pathway and acousticomotor systems: connections with the inferior colliculus. Brain Res Rev 15:295–323

Jane JA, Masterton RB, Diamond IT (1965) The function of the tectum for attention to auditory stimuli in the cat. J Comp Neurol 125:165–191

Jen PH, Chen QC, Sun XD (1998) Corticofugal regulation of auditory sensitivity in the bat inferior colliculus. J Comp Physiol A 183:683–697

Ji J, Wise KD (1992) An implantable CMOS circuit interface for multiplexed microelectrode recording arrays. IEEE J Solid-State Circuits 27:433–443

Kelly JP, Wong D (1981) Laminar connections of the cat's auditory cortex. Brain Res 212:1–15

Klinke R, Kral A, Heid S, Tillein J, Hartmann R (1999) Recruitment of the auditory cortex in congenitally deaf cats by long-term cochlear electrostimulation. Science 285:1729–1733

Kral A, Hartmann R, Tillein J, Heid S, Klinke R (2002) Hearing after congenital deafness: a central auditory plasticity and sensory deprivation. Cereb Cortex 12:797–807

Langner G, Wallhauser-Franke E (1999) Computer simulation of a tinnitus model based on labelling of tinnitus activity in the auditory cortex. In: Hazell JWP (ed) Proceedings of the 6th International Tinnitus Seminar. Hawthorn, Harleston, pp 132–135

Ma X, Suga N (2001a) Plasticity of bat's central auditory system evoked by focal electric stimulation of auditory and/or somatosensory cortices. J Neurophysiol 85:1078–1087

Ma X, Suga N (2001b) Corticofugal modulation of duration-tuned neurons in the midbrain auditory nucleus in bats. Proc Natl Acad Sci USA 98:14060–14065

Mensinger AF, Anderson DJ, Buchko CJ, Johnson MA, Martin DC, Tresco PA, Silver RB, Highstein SM (2000) Chronic recording of regenerating VIIIth nerve axons with a sieve electrode. J Neurophysiol 83:611–615

Muhlnickel W, Elbert T, Taub E, Flor H (1998) Reorganization of auditory cortex in tinnitus. Proc Natl Acad Sci USA 95:10340–10343

Najafi K, Wise KD, Mochizuki T (1985) A high-yield IC-compatible multichannel recording array. IEEE Trans Electron Devices 32:1206–1211

Oliver DL, Winer JA, Beckius GE, Saint Marie RL (1994) Morphology of GABAergic neurons in the inferior colliculus of the cat. J Comp Neurol 340:27–42

Redies H, Sieben U, Creutzfeldt OD (1989) Functional subdivisions in the auditory cortex of the guinea pig. J Comp Neurol 282:473–488

Saldana E, Feliciano M, Mugnaini E (1996) Distribution of descending projections from primary auditory neocortex to inferior colliculus mimics the topography of intracollicular projections. J Comp Neurol 371:15–40

Sakai M, Suga N (2001) Plasticity of cochleotopic (frequency) map in specialized and nonspecialized auditory cortex. Proc Natl Acad Sci USA 98:3507–3512

Shneiderman A, Oliver DL, Henkel CK (1988) Connections of the dorsal nucleus of the lateral lemniscus: an inhibitory parallel pathway in the ascending auditory system? J Comp Neurol 276:188–208

Suga N, Gao E, Zhang Y, Ma X, Olsen JF (2000) The corticofugal system for hearing: recent progress. Proc Natl Acad Sci USA 97:11807–11814

Sun X, Jen PHS, Sun D, Zhang S (1989) Corticofugal influences on the responses of bat inferior collicular neurons to sound stimulation. Brain Res 495:1–8

Syka J (2002) Plastic changes in the central auditory system after hearing loss, restoration of function, and during learning. Physiol Rev 82:601–636

Syka J, Popelar J (1984) Inferior colliculus in the rat: neuronal responses to stimulation of the auditory cortex. Neurosci Letters, 51:235–240.

Syka J, Popelar J, Druga R, Vlkova A (1988) Descending central auditory pathway- structure and function. In: Syka J, Masterton RB (eds) Auditory pathway, structure and function. Plenum Press, New York, pp 279–292

Torterolo P, Zurita P, Pedemonte M, Vellut RA (1998) Auditory cortical efferent actions upon inferior colliculus unitary activity in the guinea pig. Neurosci Letters 249:172–176

Winer JA, Larue DT, Diehl JJ, Hefti BJ (1998) Auditory cortical projections to the cat inferior colliculus. J Comp Neurol 400:147–174

Winer JA, Chernock ML, Larue DT, Cheung SW (2002) Descending projections to the inferior colliculus from the posterior thalamus and the auditory cortex in rat, cat, and monkey. Hear Res 168:181–195

Yan J, Ehret G (2001) Corticofugal reorganization of the midbrain tonotopic map in mice. Neuroreport 2:3313–3316

Yan J, Ehret G (2002) Corticofugal modulation of midbrain sound processing in the house mouse. Eur J Neurosci 16:119–128

Yan J, Suga N (1996) Corticofugal modulation of time-domain processing of biosonar information in bats. Science 273:1100–1103

Yan J, Suga N (1999) Corticofugal amplification of facilitative auditory responses of subcortical combination-sensitive neurons in the mustached bat. J Neurophysiol 81:817–824

Yan W, Suga N (1998) Corticofugal modulation of the midbrain frequency map in the bat auditory system. Nat Neurosci 1:54–58

Zhang Y, Suga N (1997) Corticofugal amplification of subcortical responses to single-tone stimuli in the mustached bat. J Neurophysiol 78:3489–3492

Zhang Y, Suga N (2000) Modulation of responses and frequency tuning of thalamic and collicular neurons by cortical activation in mustached bats. J Neurophysiol 84:325–333

Zhang Y, Suga N, Yan J (1997) Corticofugal modulation of frequency processing in the bat auditory system. Nature 387:900–903

Zhou X, Jen PHS (2000) Corticofugal inhibition compresses all types of rate-intensity functions of inferior collicular neurons in the big brown bat. Brain Res 881:62–68